Heavy Higgs boson production and decay via $e^+e^- \to ZH^0 \to b\bar{b}ZZ$ and irreducible backgrounds at the Next Linear Collider

Stefano Moretti*
Dipartimento di Fisica Teorica, Università di Torino, and INFN, Sezione di Torino, Via Pietro Giuria 1, 10125 Torino, Italy
and Department of Physics, University of Durham, South Road, Durham DH1 3LE, United Kingdom
(Received 2 March 1995)

The complete matrix element for $e^+e^- \to b\bar{b}ZZ$ has been computed at tree level and applied to ZH^0 production followed by $Z \to b\bar{b}$ and $H^0 \to ZZ$, including all the irreducible background, at the Next Linear Collider. We find that, assuming flavor identification of the Z-decay products, this channel, together with $e^+e^- \to b\bar{b}W^+W^-$ in which $ZH^0 \to (b\bar{b})(W^+W^-)$, can be important for the study of the parameters of the standard model Higgs boson over the heavy mass range $2M_Z \lesssim M_{H^0} \lesssim 2m_t$.

PACS number(s): 14.80.Bn, 13.38.Dg, 14.65.Fy, 14.70.Hp

INTRODUCTION

Despite the innumerable phenomenological successes of the standard model (SM), an essential ingredient is still missing: the discovery of the Higgs boson H^0. This particle plays a crucial role in generating the spontaneous symmetry breaking of the $SU(2)_L \times U(1)_Y$ gauge group of the electroweak interactions, and in ensuring the renormalizability of the whole theory. We know that the H^0 is supposed to be a CP-even neutral scalar boson, we know its couplings to the other elementary particles, but no prediction on its mass (i.e., M_{H^0}) can theoretically be done.

However, an upper bound of approximately 1 TeV (from perturbative unitarity arguments [1]) is expected, whereas a lower limit can be derived from current experiments at LEP I. In fact, from unsuccessful searches for $e^+e^- \to Z \to Z^*H^0$ events at the Z peak, one can deduce the bound $M_{H^0} \gtrsim 60$ GeV [2].

Assuming the above mass range, various studies on the feasibility of its detection by the next generation of high energy machines have been carried out, both at hadron colliders [3–6] and at the e^+e^- ones [3,7–11].

On the basis of the expected center-of-mass (c.m.) energies, luminosities, detector performances of these accelerators, and of the predicted cross sections and branching ratios, it has been definitely demonstrated that, if the H^0 is in the mass region $M_{H^0} \lesssim M_Z$ (i.e., light Higgs boson), it can be discovered at LEP II (with $\sqrt{s_{ee}} = 160$–200 GeV) in a large variety of channels [7]. For a larger mass Higgs boson, a pp collider like the LHC ($\sqrt{s_{pp}} = 14$ TeV) and/or an e^+e^- accelerator like the Next Linear Collider (NLC, with $\sqrt{s_{ee}} = 300$–1000 GeV) is needed. Even though at the LHC the mass range $M_z \lesssim M_{H^0} \lesssim 130$ GeV is quite difficult to cover since in this case the Higgs boson mainly decays to $b\bar{b}$ pairs (signature which has a huge QCD background if b quarks cannot be recognized), nevertheless, it should be possible to detect it in the rare $\gamma\gamma$-decay mode [12] via the associated production with a $W^\pm$ boson [13,14] or a $t\bar{t}$ pair [15,16]. At the LHC, for $M_{H^0} \gtrsim 130$ GeV, the "gold-plated" four-lepton mode (i.e., $H^0 \to ZZ \to l^+l^-l^+l^-$), via various production channels, remains the clearest signature [4,5]. At NLC's, with $\sqrt{s_{ee}} = 300$–500 GeV, the Higgs boson detection is possible over the whole intermediate mass range (i.e., $M_Z \lesssim M_{H^0} \lesssim 2M_{W^\pm}$) [17], via the bremsstrahlung reaction $e^+e^- \to Z^* \to ZH^0$ [18] and/or the fusion processes $e^+e^- \to \bar{\nu}_e\nu_e W^{\pm *}W^{\mp *}(e^+e^-Z^*Z^*) \to \bar{\nu}_e\nu_e(e^+e^-)H^0$ [19]. If $\sqrt{s_{ee}} \gtrsim 500$ GeV, a heavy Higgs boson (i.e., $M_{H^0} \gtrsim 2M_{W^\pm}$, and mainly produced via the fusion processes), can be detected via the four-*jet* modes $H^0 \to W^\pm W^\mp, ZZ \to jjjj$ as well as via the $4l$ decay [20,21]. Finally, signatures that can be disentangled through b tagging [22] must also be added to the mentioned channels: such as, e.g., at the LHC, $t\bar{t}H^0$ production, with one $t(\bar{t})$ decaying semileptonically and $H^0 \to b\bar{b}$, with 80 GeV $\lesssim M_{H^0} \lesssim 130$ GeV [23].

In a recent study [24], we presented an analysis of the Bjorken reaction $e^+e^- \to ZH^0$ in the case of a heavy Higgs boson decaying to W^+W^--pairs and with $Z \to b\bar{b}$, and of all the $b\bar{b}W^+W^-$ irreducible background, assuming flavor identification of the Z-decay products. We emphasized in that work the importance of b tagging the weak boson Z as this could be one of the most efficient ways of detecting it, since this channel is free from $W^\pm$-decay backgrounds, has a branching ratio approximately five times larger than the $Z \to l^+l^-$ channel (with $l = e$, μ, or τ), and is comparable to the fraction of invisible decays $Z \to \nu\bar{\nu}$.

In Ref. [24] we found that, after carrying a missing mass analysis [26] on $e^+e^- \to b\bar{b}W^+W^-$, there are values of the Higgs boson mass for which a simple cut on the invariant mass $M_{b\bar{b}}$ is sufficient in order to completely eliminate the irreducible background (which is dominated by $t\bar{t}$ production and decay) when the double distributions

*Electronic address:
Moretti @to.infn.it; Stefano.Moretti@durham.ac.uk

$d\sigma/dM_{b\bar{b}}/dM_{W^+W^-}$ of signal and background events do not overlap in the plane $(M_{b\bar{b}}, M_{W^+W^-})$. Otherwise, further cuts based on the kinematics of the $t\bar{t}$ background are needed, and these still maintain an acceptable number of events from Higgs boson production.

The missing mass method has the attractive feature of being independent of assumptions about the H^0-decay modes and of tagging the decay products of the Z produced via the Bjorken reaction only. Applied to the two-to-two body process $e^+e^- \to ZH^0$ it provides a very efficient experimental technique to detect the Higgs boson scalar or to rule out this particle with certainty. Moreover, it allows to measure the branching ratios of the Higgs boson: in fact, once the total "inclusive" rates obtained from the missing mass analysis are known, by studying the Higgs boson decay channels exclusively it is possible to deduce the corresponding branching fractions. Finally, this technique is particularly important, e.g., in the minimal supersymmetric extension of the standard model (MSSM), if $M_\chi < M_h/2$ (χ represents a neutralino and h the lightest MSSM neutral scalar boson). In fact, in this case, the "invisible" decay $h \to \chi\chi$ is the dominant decay channel in the intermediate range of M_h. However, by missing mass analyses, the signal $e^+e^- \to Zh \to (l^+l^-)(\chi\chi)(l = e \text{ or } \mu)$ should clearly appear as a peak in the recoiling mass distribution [27].

In the SM, for $M_{H^0} \gtrsim 2M_{W^\pm}$, as the $b\bar{b}W^+W^-$ events enter in the missing mass distribution so should the $b\bar{b}ZZ$ ones, and with a quite large component of signal $H^0 \to ZZ$ if compared to $H^0 \to W^+W^-$, since the ZZ-branching ratio is only a factor of two/three less than the W^+W^- one in the heavy Higgs boson mass region (with $M_{H^0} \lesssim 2m_t$). Because of this "inclusive" analysis on the decay products of the Higgs boson, both signals and irreducible backgrounds of both the above processes must be then considered at the same time.[1] Therefore, we believe that a complete study, which includes $e^+e^- \to b\bar{b}ZZ$ as well as $e^+e^- \to b\bar{b}W^+W^-$, is needed in order to definitely establish the feasibility of all the foreseen measurements of the Higgs boson parameters, if the missing mass analysis is adopted and the Z is assumed to decay to $b\bar{b}$ pairs, with these tagged by vertex detectors.

As already done in Ref. [24] we do not include in our computations the beam energy spread from bremsstrahlung and beamsstrahlung effects. As a result, one has to expect the true number of events to be slightly higher than the number we predict here.

In this paper, using the full matrix element for the process $e^+e^- \to b\bar{b}ZZ$ we study the production of a heavy SM Higgs boson (i.e., $M_{H^0} \geq 2M_{W^\pm}$) via the Bjorken bremsstrahlung reaction $e^+e^- \to ZH^0$, followed by the decays $Z \to b\bar{b}$ and $H^0 \to ZZ$, and of all the irreducible $b\bar{b}ZZ$ background. Moreover, we present final results in which both the rates for $b\bar{b}W^+W^-$ and $b\bar{b}ZZ$ are added together.

Following the track of Ref. [24], we give details of the calculation in Sec. II, while in Sec. III we present and discuss the results. Finally, Sec. IV is devoted to our conclusions.

CALCULATION

All the Feynman diagrams describing the process $e^+e^- \to b\bar{b}ZZ$ at tree level are shown in Fig. 1, where graphs in which Z's can be exchanged (i.e., when they do not come from the same vertex) must be counted twice (exchanging the corresponding four-momenta). The matrix element has been computed using the method of Ref. [28] and we have checked the FORTRAN code for BRS invariance [29] and compared it with a second one, produced by MadGraph [30] and using the package HELAS [31].[2]

The following numerical values of the parameters were adopted: $M_Z = 91.1$ GeV, $\Gamma_Z = 2.5$ GeV, $\sin^2(\theta_W) = 0.23$, $m_b = 5.0$ GeV, and $\alpha_{em} = 1/128$. For the Higgs boson width (i.e., Γ_{H^0}) we have adopted the tree-level expression, and we have not included effects of the width of the final state Z's.

A few thoughts will now be devoted to the procedure adopted for the integration of the matrix element over the phase space. In order to control the interplay between the various peaks which appear in the integration domain when all tree-level contributions are kept into account, we have split the Feynman amplitude squared into a sum of different (non-gauge-invariant) terms, each of which corresponds to the modulus squared of the resonant diagrams (for each possible resonance) and, eventually, their interference with other channels [24]. In a similar way, the contribution of nonresonant diagrams must also be considered.

Explicitly, in the case of the process $e^+e^- \to b\bar{b}ZZ$ with $M_{H^0} > 2M_Z$, we have $H^0 \to b\bar{b}Z$, $Z \to b\bar{b}$, $H^0 \to ZZ$, $ZH^0 \to (b\bar{b})(ZZ)$, and $H^0 \to b\bar{b}$ resonances, via the five channels (see Fig. 1):[3]

$$M_1: \quad H^0 \to b\bar{b}Z \quad \text{diagrams } 11, 12, 18,$$

$$M_2: \quad Z \to b\bar{b} \quad \text{diagrams } 4, 5, 6 (\text{with } Z \text{ propagators}),$$

$$M_3: \quad H^0 \to ZZ \quad \text{diagrams } 15, 16,$$

$$M_4: \quad ZH^0 \to (b\bar{b})(ZZ) \quad \text{diagram } 17,$$

$$M_5: \quad H^0 \to b\bar{b} \quad \text{diagrams } 13, 14.$$

Diagrams 1–3, 7–10, and 4–6 (with γ propagators) constitute the sixth (nonresonant) channel (M_6). Obviously,

[1] Moreover, in the range $2M_{W^\pm} \lesssim M_{H^0} \lesssim 2m_t$, $H^0 \to W^+W^-$ and $H^0 \to ZZ$ are the only relevant branching fractions.

[2] Running then only the first one for producing results.

[3] Diagrams with exchanged Z's are here implied.

if M_i indicates the sum of the diagrams entering in the ith channel, one has

$$M_{\rm tot} = \sum_{i=1}^{6} M_i \ , \tag{1}$$

where $M_{\rm tot}$ is the total Feynman amplitude. In squaring Eq. (1) we take the combinations[4]

$$\mathcal{M}_1^2 = |M_1|^2, \mathcal{M}_2^2 = |M_2|^2 + 2\,{\rm Re}[M_2 M_4^*] \ , \tag{2}$$

$$\mathcal{M}_3^2 = |M_3|^2 + 2\,{\rm Re}[M_3 M_4^*] \ , \tag{3}$$

$$\mathcal{M}_4^2 = |M_4|^2 \ , \quad \mathcal{M}_5^2 = |M_5|^2 \ , \tag{4}$$

$$\begin{aligned}\mathcal{M}_6^2 = {} & |M_6|^2 + 2\,{\rm Re}[M_1 M_2^*] + 2\,{\rm Re}[M_1 M_3^*] + 2\,{\rm Re}[M_1 M_4^*] + 2\,{\rm Re}[M_1 M_5^*] \\ & + 2{\rm Re}[M_1 M_6^*] + 2\,{\rm Re}[M_2 M_3^*] + 2\,{\rm Re}[M_2 M_5^*] + 2\,{\rm Re}[M_2 M_6^*] \\ & + 2\,{\rm Re}[M_3 M_5^*] + 2\,{\rm Re}[M_3 M_6^*] + 2\,{\rm Re}[M_4 M_5^*] + 2\,{\rm Re}[M_4 M_6^*] + 2\,{\rm Re}[M_5 M_6^*] \ , \end{aligned} \tag{5}$$

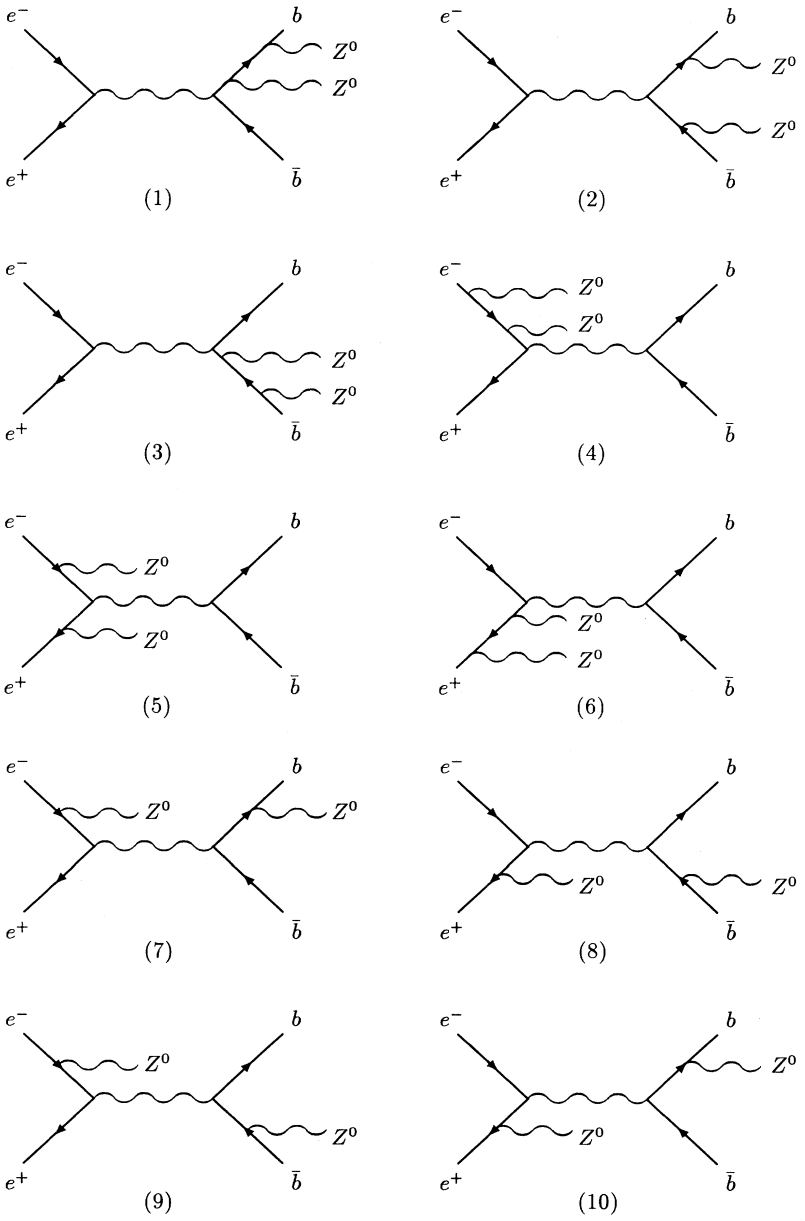

FIG. 1. Feynman diagrams contributing in the lowest order to $e^+e^- \to b\bar{b}Z^0Z^0$ (those ones obtainable by exchanging the two Z^0 bosons are not shown). Internal wavy lines represent a γ or a Z^0, as appropriate. Internal dashed lines represent a Higgs boson.

[4]This in order to minimize the errors coming from the multidimensional integrations over the phase space, when we need to integrate interferences between channels with and without (or different) resonances.

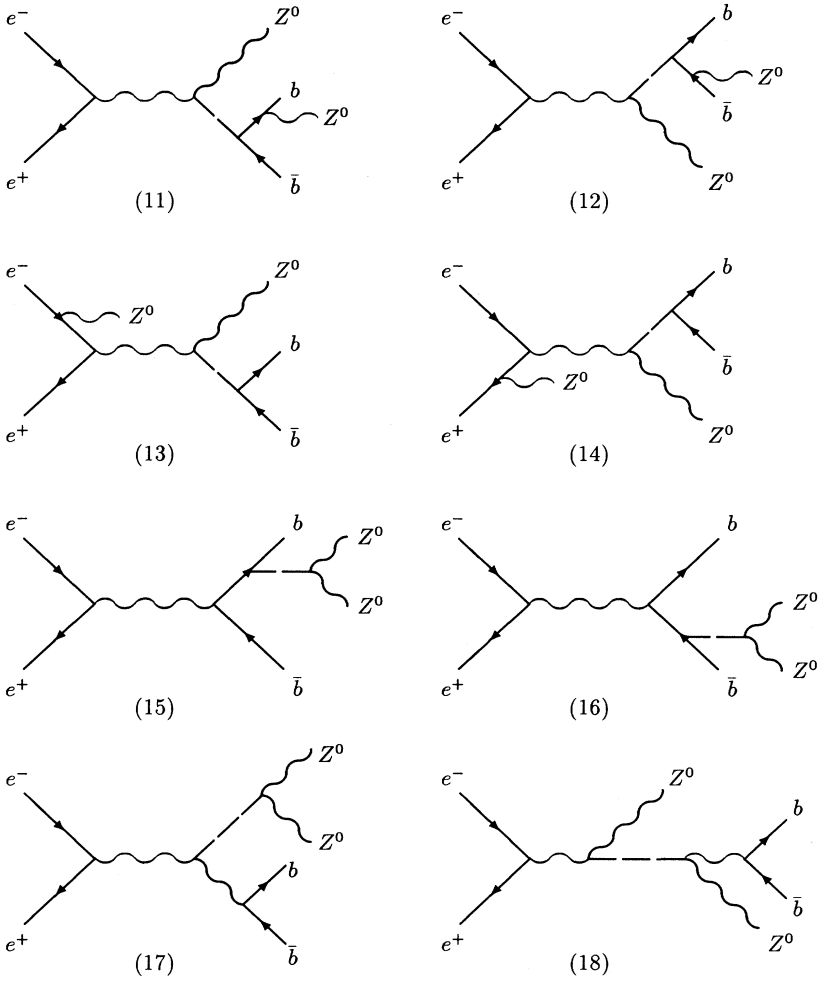

FIG. 1 *(Continued).*

where $\mathrm{Re}(x)$ represents the real part of x, and with

$$|M_{\mathrm{tot}}|^2 = \sum_{i=1}^{6} \mathcal{M}_i^2 \ , \tag{6}$$

where $|M_{\mathrm{tot}}|^2$ is the total Feynman amplitude squared.

Then, to obtain an integrand function smoothly dependent on the integration variables, for each contribution in the matrix element (6) containing a resonance we make the change

$$P^2 - M^2 = M\Gamma \tan\theta \ , \tag{7}$$

this factorizes the Jacobian

$$dp^2 = \frac{1}{M\Gamma}[(p^2 - M^2)^2 + M^2\Gamma^2]d\theta \ , \tag{8}$$

which removes the dependence on the Breit-Wigner peaks appearing in the $\mathcal{M}_i^2$ terms. Here, p, M, and Γ stand for the four-momentum, the mass, and the width of the resonance, respectively. Then, we separately integrated the various contributions (2)–(5) by VEGAS [32], using an appropriate phase space for each.

Finally, throughout this paper we adopt an integrated luminosity $\mathcal{L} = 10\ \mathrm{pb}^{-1}$ and we assume that only one b jet is tagged, with an efficiency $\epsilon_b = 1/3$ (i.e., ϵ_b is the probability for a b quark to satisfy a given set of tagging requirements). Therefore, the probability of tagging at least one $b(\bar{b})$ out of a $b\bar{b}$ pair is $P_1 = 1-(1-\epsilon_b)^2 = 5/9 \approx 0.56$.[5] In principle, we should consider here the fact that there are also the other two Z's in the event, one or both of which can decay to $b\bar{b}$ pairs. To this aim, we express $P_n = 1 - (1-\epsilon_b)^{2n}$ to be the probability of tagging at least one $b(\bar{b})$ out of n $b\bar{b}$ pairs, and we "roughly" split the cross section $\sigma(e^+e^- \to b\bar{b}ZZ)$ into three contributions: $\sigma_3 = \sigma(e^+e^- \to b\bar{b}ZZ) \times [B(Z \to b\bar{b})]^2 \times \left(\frac{\delta_{b\bar{b},b\bar{b},b\bar{b}}}{\delta_{ZZ}}\right)$, $\sigma_2 = \sigma(e^+e^- \to b\bar{b}ZZ) \times [2B(Z \to b\bar{b})] \times \left(\frac{\delta_{b\bar{b},b\bar{b}}}{\delta_{ZZ}}\right)$, and $\sigma_1 = \sigma(e^+e^- \to b\bar{b}ZZ) - \sigma_2 - \sigma_3$, corresponding to the case of three, two, and one final $b\bar{b}$ pairs

[5]We notice how this assumption implies rather loose identification requirements on b jets, since for a standard configuration of a NLC detector with one *jet* having at least three charged particle tracks with a significant impact parameter (see, e.g., Ref. [25] for full details), more than 3/4 of the b-tagged events in $Z \to jj$ decays are genuine $Z \to b\bar{b}$ events.

from Z decays, respectively. Here, $B(Z \to b\bar{b}) \approx 0.15$ is the Z-branching ratio into b quarks, whereas $\delta_{ZZ}(\delta_{b\bar{b},b\bar{b}})[\delta_{b\bar{b},b\bar{b},b\bar{b}}] = 1/2(1/4)[1/36]$ is the $1/k!$ factor for each k-uple of identical particles (since we integrated over the whole phase space) in $b\bar{b}XY(b\bar{b}b\bar{b}X)[b\bar{b}b\bar{b}b\bar{b}]$ final states, with X and Y not representing b particles. Then, we expect the efficiency of tagging at least one $b(\bar{b})$ out of all the possible final signatures of $b\bar{b}ZZ$ events to be $P_{\rm tot} \approx \sum_{n=1}^{3} P_n \sigma_n/\sigma(e^+e^- \to b\bar{b}ZZ) \approx 0.59$. Since adopting one or the other of the two values P_1 and $P_{\rm tot}$ would not change the conclusions (see later on), as a first approximation we forget the complications due to possible $b\bar{b}$ decays of the on-shell Z's in $b\bar{b}ZZ$ events, and we continue to treat these latter "inclusively."[6]

RESULTS

Our results are presented throughout Figs. 2–7, and in Tables I–IV.

In Figs. 2 and 3 we show the differential distribution $d\sigma/dM_{ZZ}$ for $e^+e^- \to b\bar{b}ZZ$ events, obtained from the full matrix element (i.e., summed over all the six contributions $\mathcal{M}_i^2$), for two different values of the c.m. energy of a NLC, and for the same choice of Higgs boson masses adopted in Ref. [24] (see Figs. 3 and 4 there).[7] As in Ref. [24], in order to disentangle the signal $ZH^0 \to (b\bar{b})(ZZ)$ from the irreducible background we have imposed a cut around the Z mass, requiring that $|M_Z - M_{b\bar{b}}| < 10$ GeV. Also, since we are looking for events that have to be tagged by microvertex detectors, we selected only configurations with $|\cos\theta_{b\bar{b}}| < 0.8$ [25,26].

Both in Fig. 2 and in Fig. 3 the $H^0 \to ZZ$ peaks appear clearly visible over the flat structure of the irreducible background, which [looking at the integrals of the various components (2)–(5) of the matrix element] appears to be dominated by the $H^0 \to b\bar{b}Z$ (i.e., $\mathcal{M}_1^2$) and the $Z \to b\bar{b}$ (i.e., $\mathcal{M}_2^2$) contributions, which, obviously, largely pass the cut in $M_{b\bar{b}}$. Moreover, the cross section corresponding to $\mathcal{M}_1^2$ is roughly equal to twice the signal (i.e., the integral of $\mathcal{M}_4^2$) since these two processes can be approximated in terms of a *production* $\times$ *decay* reaction $e^+e^- \to ZH^0 \to Z(ZZ) \times B(Z \to b\bar{b})$, with the $Z \to b\bar{b}$ decay corresponding, in one case, to a Z directly coming from the two-body Bjorken process (diagram 17) and, in the other case, to a Z from the $H^0 \to ZZ$ decay (diagrams 18), and with difference (only a few fractions of picobarns for the integrated "cross sections") coming from the different kinematics of the decaying Z's.[8] The factor of 2 comes from having two Z's in the $\mathcal{M}_1^2$ contri-

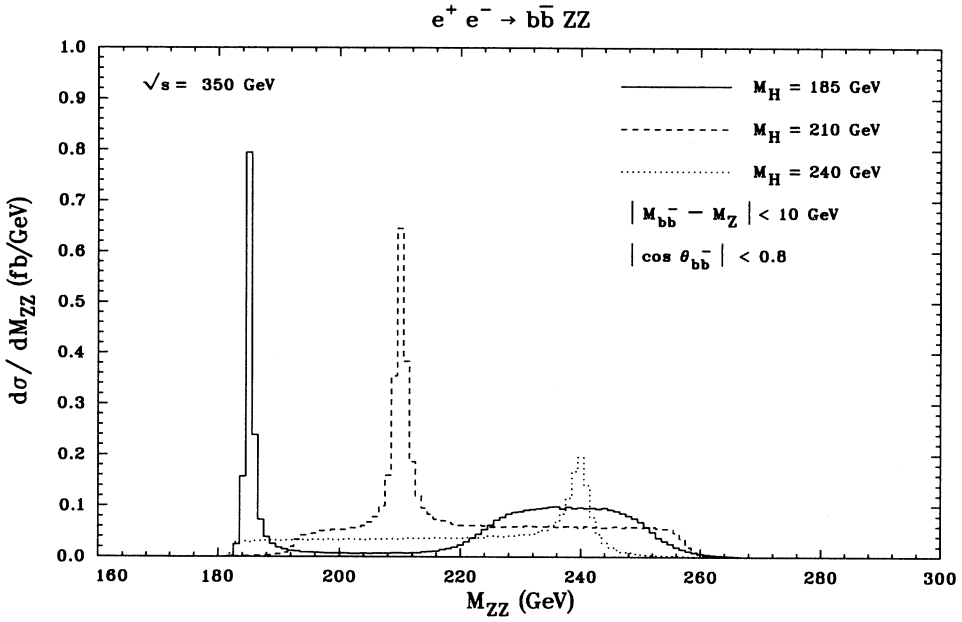

FIG. 2. The differential distribution $d\sigma/dM_{Z^0Z^0}$ for $e^+e^- \to b\bar{b}Z^0Z^0$ (full matrix element with all Higgs contributions), at $\sqrt{s} = 350$ GeV, for $M_{H^0} = 185$ GeV (continuous line), $M_{H^0} = 210$ GeV (dashed line), and $M_{H^0} = 240$ GeV (dotted line), with the following cuts: $|M_{Z^0} - M_{b\bar{b}}| < 10$ GeV and $|\cos\theta_{b\bar{b}}| < 0.8$.

[6]Also, throughout the analysis we implicitly assume that we are always considering the right "$b\bar{b}$" pair [i.e., the tagged $b(\bar{b})$ with the untagged $\bar{b}(b)$ coming from the same Z], this is due to the underlying cut in $M_{b\bar{b}}$, which drastically suppresses (because of the narrowness of the Z resonance) any contribution coming from wrong $b(\bar{b})$-jet combinations, with the jet eventually coming from Z decays (as done in Ref. [24]).

[7]Only the value $M_{H^0} = 170$ GeV, there considered at $\sqrt{s} = 350$ GeV, has been dropped here, since this case would correspond to a below threshold decay $H^0 \to Z^*Z^* \to f\bar{f}f'\bar{f}'$ (where $f^{(\prime)}$ stands for a lepton l or ν_l, with $l = e, \mu, \tau$, or a light quark $q = u, d, s, c, b$), with a six particle signature $(b\bar{b})(f\bar{f})(f'\bar{f}')$, which deserves a more complicated treatment than of the one we are interested in performing here.

[8]In the following we will speak of a "prompt Z" for the case $\mathcal{M}_4^2$ and of a "H^0-decay Z" for $\mathcal{M}_1^2$. Also we will write "bremsstrahlung Z" when we will intend to indicate a Z produced via the diagrams entering in $\mathcal{M}_2^2$.

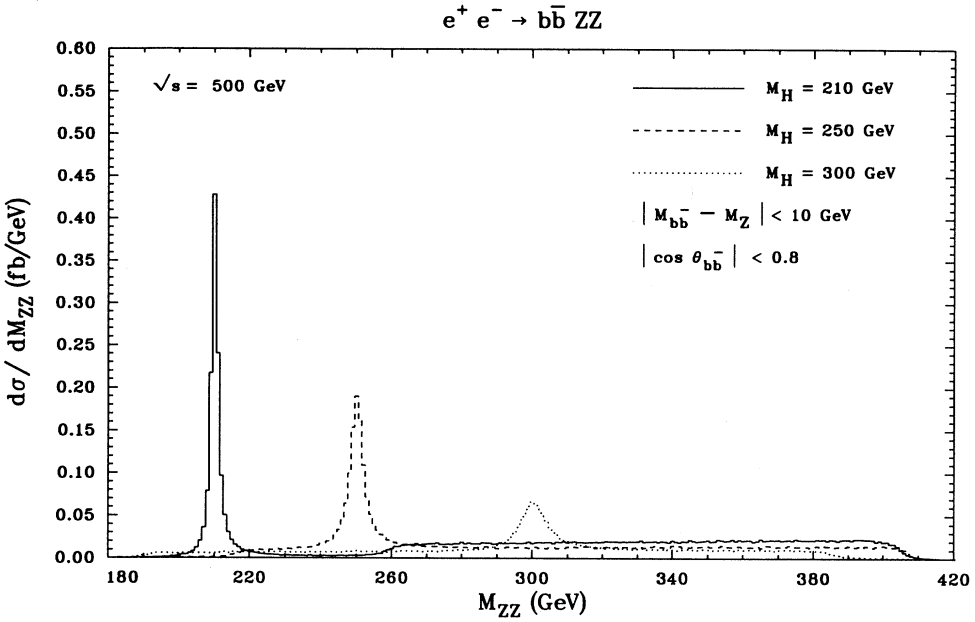

FIG. 3. The differential distribution $d\sigma/dM_{Z^0Z^0}$ for $e^+e^- \to b\bar{b}Z^0Z^0$ (full matrix element with all Higgs contributions), at $\sqrt{s} = 500$ GeV, for $M_{H^0} = 210$ GeV (continuous line), $M_{H^0} = 250$ GeV (dashed line), and $M_{H^0} = 300$ GeV (dotted line), with the following cuts: $|M_{Z^0} - M_{b\bar{b}}| < 10$ GeV and $|\cos\theta_{b\bar{b}}| < 0.8$.

bution that can both decay to a $b\bar{b}$ pair. In the case of $\mathcal{M}_2^2$ we have three Z's produced via bremsstrahlung off the e^+e^- fermion line, with one of them decaying to the $b\bar{b}$ pair.[9]

In Table I we present the expected number of signal (S) and background (B) events together with the statistical significance $S/\sqrt{B}$, for $\mathcal{L} = 10$ fb^{-1} and $\epsilon_b = 1/3$, in a window of 10 GeV around the adopted values of the Higgs boson mass M_{H^0}, at $\sqrt{s} = 350$ and 500 GeV, after the cuts in $M_{b\bar{b}}$ and $\cos\theta_{b\bar{b}}$ discussed above. Here and in the following tables the signal represents the resonant contribution $e^+e^- \to ZH^0 \to (b\bar{b})(VV)$ ($V = Z$ and/or $W^\pm$), whereas by background we mean the cross section obtained from all diagrams without the Higgs boson (see also Ref. [24]). Looking at the ratio $S/\sqrt{B}$ it would seem that, even though with a small number of events in some instances, the signal is detectable. However, we have to remember that the final goal is to look at the spectrum in missing mass and at the total number of events when the rates for both signal and background of both the processes $e^+e^- \to b\bar{b}ZZ$ and $e^+e^- \to b\bar{b}W^+W^-$ are added together in an inclusive analysis. For that, we have plotted in Figs. 4 and 5 the differential distribution $d\sigma/dM_{VV}$, which is the sum of the corresponding histograms of the two above processes (when $VV = ZZ$ and $W^\pm W^\mp$), for the usual combination of Higgs boson masses and c.m. energies [i.e., we sum the distributions in Fig. 3(4) of [24] and in Fig. 2(3) of this study]. Then we have again integrated these curves in a window of 10 GeV around M_{H^0}, obtaining the total number of signal and background events (now picked out of the inclusive missing mass spectrum) and the corresponding significancies shown in Table II.[10]

From Figs. 4 and 5 and Table II it is then clear

TABLE I. The expected number of $e^+e^- \to b\bar{b}Z^0Z^0$ signal and background events in the window $|M_{H^0} - M_{Z^0Z^0}| < 5$ GeV and their statistical significance at $\sqrt{s} = 350$ and 500 GeV for a selection of Higgs masses after the cuts: $|M_{Z^0} - M_{b\bar{b}}| < 10$ GeV and $|\cos\theta_{b\bar{b}}| < 0.8$. We assume that only one b jet is tagged with efficiency $\epsilon_b = 1/3$. The luminosity is taken to be $\mathcal{L} = 10$ fb^{-1}.

M_{H^0} (GeV)	Signal	Background	$S/\sqrt{B}$
	$\sqrt{s} = 350$ GeV		
185	7.45	0.18	17.63
210	9.00	3.64	4.72
240	4.44	1.13	4.17
	$\sqrt{s} = 500$ GeV		
210	6.78	0.058	28.20
250	4.93	0.73	5.75
300	2.51	0.51	3.52
	$\mathcal{L} = 10$ fb^{-1} $\epsilon_b = 1/3$		

[9]We wonder if the case $\mathcal{M}_1^2$ has to be really considered as a background, since it includes a Higgs boson produced via the Bjorken reaction, even though not peaking in the missing mass spectrum: in fact not all the particles entering in the missing mass come from the H^0. By the way, its spectrum in this variable is quite flat and completely useless in disentangling H^0 signals with respect to the other backgrounds.

[10]Since in [24] only the significancies for the cases $\sqrt{s} = 500$ GeV and $M_{H^0} = 250$ and 300 GeV were given for the value of *top* mass here adopted, we list now the remaining ones: they are 8.50(8.36)[6.20] for $\sqrt{s} = 350$ GeV and $M_{H^0} = 185(210)$ [240] GeV, and 17.57 for $\sqrt{s} = 500$ GeV and $M_{H^0} = 210$ GeV.

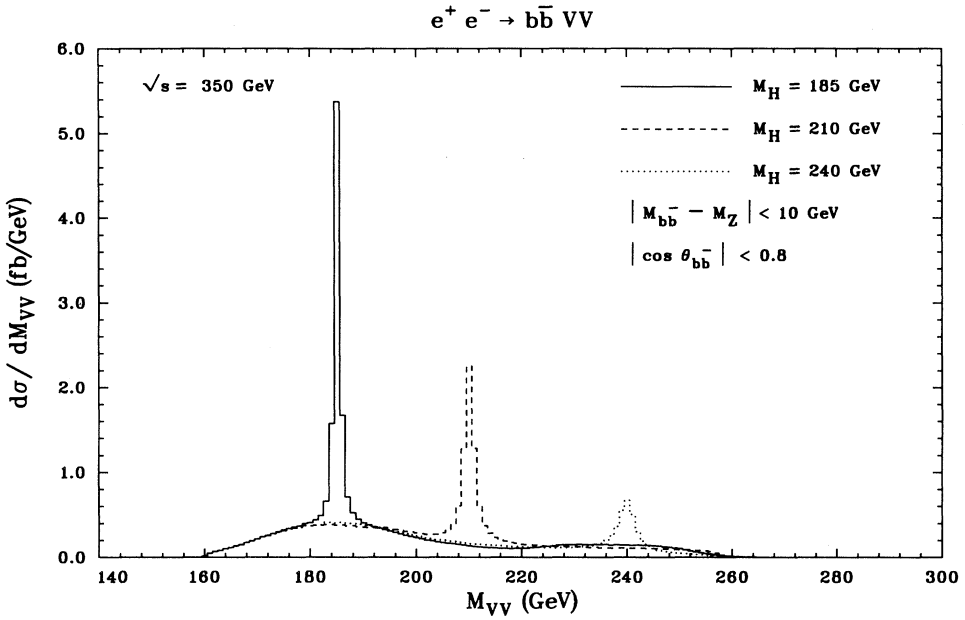

FIG. 4. The differential distribution $d\sigma/dM_{VV}$, for $e^+e^- \to b\bar{b}Z^0Z^0$ and $e^+e^- \to b\bar{b}W^+W^-$ processes (full matrix elements with all Higgs contributions), added together, at $\sqrt{s} = 350$ GeV, for $M_{H^0} = 185$ GeV (continuous line), $M_{H^0} = 210$ GeV (dashed line), and $M_{H^0} = 240$ GeV (dotted line), with the following cuts: $|M_{Z^0} - M_{b\bar{b}}| < 10$ GeV and $|\cos\theta_{b\bar{b}}| < 0.8$. Plots corresponding to the contribution of $e^+e^- \to b\bar{b}W^+W^-$ events are taken from Ref. [24] (assuming $m_t = 175$ GeV).

that adding together the missing mass spectra for the two processes increases the total significancies, to $\approx$ 18(14)[20]% for $\sqrt{s} = 350$ GeV and $M_{H^0} = 185(210)[240]$ GeV and to $\approx$ 35(36)[43]% for $\sqrt{s} = 500$ GeV and M_{H^0}=210(250)[300] GeV, with respect to those ones obtained for the process $e^+e^- \to b\bar{b}W^+W^-$ only [24]. Now, with the values of Table II the only signal that still appears quite difficult to disentangle from the irreducible background is $M_{H^0} = 300$ GeV at $\sqrt{s} = 500$ GeV; this is also due to the fact that for this value of M_{H^0} the Higgs width is sizably large ($\Gamma_{H^0} \approx 8.5$ GeV) and comparable to the one of the window in M_{VV} we integrate over (whereas this does not happen for the other cases, since for them we always have $\Gamma_{H^0} < 4.2$ GeV, the value of Γ_{H^0} for $M_{H^0} = 250$ GeV).

Of course, at this point we could decide to integrate over a larger window, retaining then more signal, but for $\sqrt{s} = 500$ GeV and (let us say) $|M_{VV} - 300$ GeV $| \lesssim 10$ GeV we would include also the region (around $M_{VV} \approx 310$ GeV) where the background from $e^+e^- \to b\bar{b}W^+W^-$ is maximum (compare with Fig. 4 of [24]). Therefore, this is not the best way to proceed, and in fact in Ref. [24] it has instead been decided to apply cuts based on the kinematics of $t\bar{t}$ production and decay: i.e., we required that one of the $W^\pm$'s (let us say W^+) failed in reproducing the kinematics of the $t\bar{t}$-final state when coupled with either of the two b's, namely that $m_t - 10$ GeV $> |M_{W^+b(W^+\bar{b})}| > m_t + 10$ GeV and $E_{\rm beam} - 10$ GeV

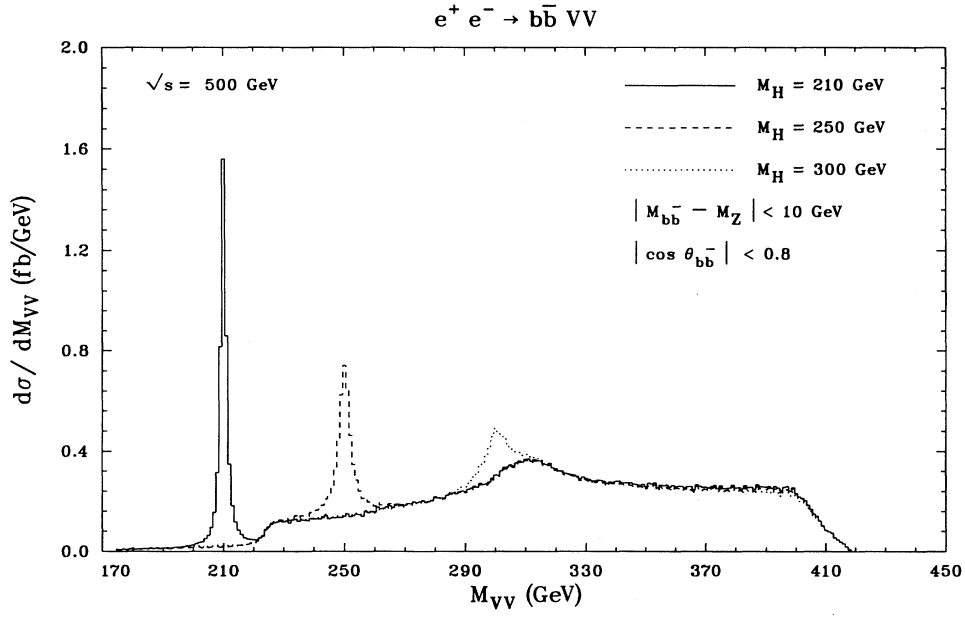

FIG. 5. The differential distribution $d\sigma/dM_{VV}$, for $e^+e^- \to b\bar{b}Z^0Z^0$ and $e^+e^- \to b\bar{b}W^+W^-$ processes (full matrix elements with all Higgs contributions), added together, at $\sqrt{s} = 500$ GeV, for $M_{H^0} = 210$ GeV (continuous line), $M_{H^0} = 250$ GeV (dashed line), and $M_{H^0} = 300$ GeV (dotted line), with the following cuts: $|M_{Z^0} - M_{b\bar{b}}| < 10$ GeV and $|\cos\theta_{b\bar{b}}| < 0.8$. Plots corresponding to the contribution of $e^+e^- \to b\bar{b}W^+W^-$ events are taken from Ref. [24] (assuming $m_t = 175$ GeV).

TABLE II. The expected number of signal and background events for $e^+e^- \to b\bar{b}Z^0Z^0$ and $e^+e^- \to b\bar{b}W^+W^-$ processes, added together, in the window $|M_{H^0} - M_{VV}| < 5$ GeV and their statistical significance at $\sqrt{s} = 350$ and 500 GeV for a selection of Higgs masses after the cuts: $|M_{Z^0} - M_{b\bar{b}}| < 10$ GeV and $|\cos\theta_{b\bar{b}}| < 0.8$. We assume that only one b jet is tagged with efficiency $\epsilon_b = 1/3$. The luminosity is taken to be $\mathcal{L} = 10$ fb^{-1}. Numbers corresponding to the contribution of $e^+e^- \to b\bar{b}W^+W^-$ events are taken from Ref. [24] (assuming $m_t = 175$ GeV).

M_{H^0} (GeV)	Signal	Backgrounds	$S/\sqrt{B}$
	$\sqrt{s} = 350$ GeV		
185	47.85	22.79	10.02
210	32.47	11.53	9.56
240	15.06	4.06	7.47
	$\sqrt{s} = 500$ GeV		
210	24.48	1.07	23.65
250	16.56	9.01	5.52
300	8.17	17.92	1.93

$\mathcal{L} = 10$ fb^{-1} $\epsilon_b = 1/3$

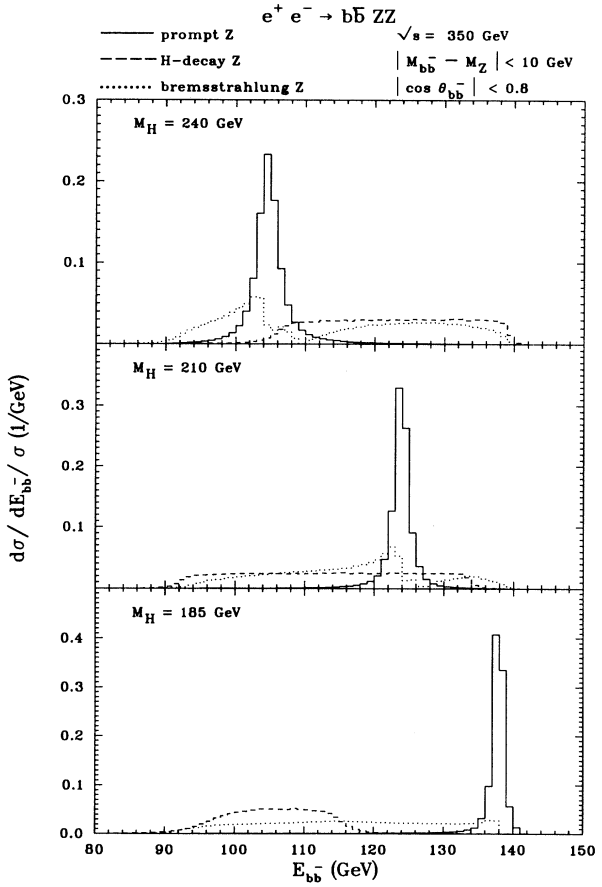

FIG. 6. The differential distribution $d\sigma/dE_{b\bar{b}}/\sigma$ for the signal $e^+e^- \to Z^0H^0$ with the $b\bar{b}$ pair coming from the prompt Z^0 (continuous line), from a H^0-decay Z^0 (dashed line) and from a bremsstrahlung Z^0 (dotted line), at $\sqrt{s} = 350$ GeV, for $M_{H^0} = 185$, 210, and 240 GeV, with the following cuts: $|M_{Z^0} - M_{b\bar{b}}| < 10$ GeV and $|\cos\theta_{b\bar{b}}| < 0.8$.

$> |E_{W^+} + E_{b(\bar{b})}| > E_{\text{beam}} + 10$ GeV. But, even though these selection criteria are quite convenient [24], they require the decay products of the $W^\pm$ to be tagged: that is, a further experimental detection effort is needed compared to the missing mass analysis which only requires tagging the $b\bar{b}$ system.

The effect of another additional cut can then be exploited. If we look at the spectrum in energy $E_{b\bar{b}}$ of the $b\bar{b}$ pair, this (due to the ZH^0 two-body kinematics of the Bjorken production) is "practically" monoenergetic, with $E_{b\bar{b}} \approx (s - M^2_{H^0} + M^2_Z)/2\sqrt{s}$, for a pair coming from a prompt Z, whereas it appears quite broad if the pair is produced by a H^0 decay or a bremsstrahlung Z (Figs. 6 and 7).[11] Therefore, retaining only events in an

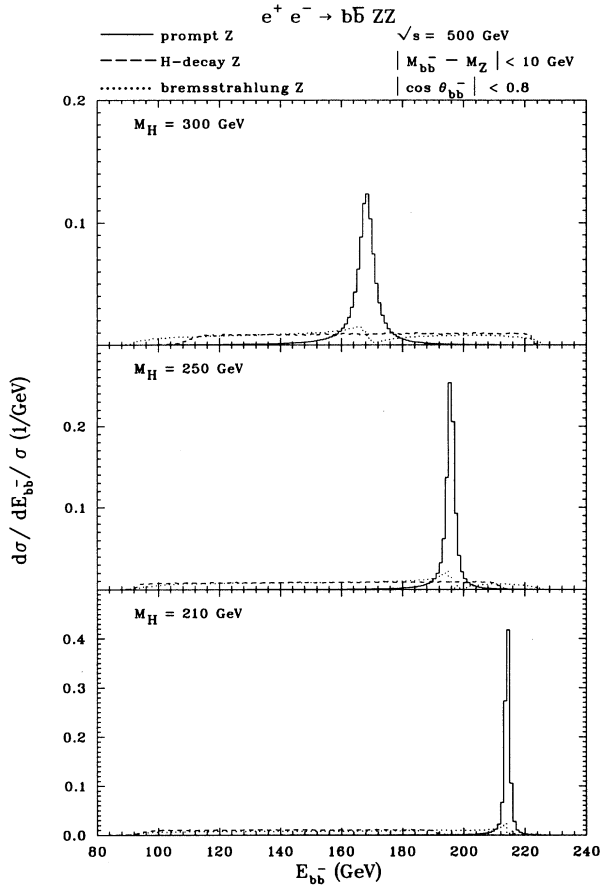

FIG. 7. The differential distribution $d\sigma/dE_{b\bar{b}}/\sigma$ for the signal $e^+e^- \to Z^0H^0$ with the $b\bar{b}$-pair coming from the prompt Z^0 (continuous line), from a H^0-decay Z^0 (dashed line) and from a bremsstrahlung Z^0 (dotted line), at $\sqrt{s} = 500$ GeV, for $M_{H^0} = 210$, 250, and 300 GeV, with the following cuts: $|M_{Z^0} - M_{b\bar{b}}| < 10$ GeV and $|\cos\theta_{b\bar{b}}| < 0.8$.

[11] Concerning the case of bremsstrahlung Z's it has to be remembered [see Eq. (2)] that $\mathcal{M}^2_2$ includes also the interference of $Z \to b\bar{b}$ with the signal $ZH^0 \to (b\bar{b})(ZZ)$, whose effects appear clearly visible in the "half" small peak below the signal one, and which, at the end, slightly enhance the contribution of this background.

appropriate window around the maximum in $E_{b\bar{b}}$ could further reduce the two Z resonant backgrounds (and not those only) with respect to the signal. Some care has to be taken in exploiting this possibility. In fact, the above spectrum is really monoenergetic only apart from photon bremsstrahlungs off e^+e^--lines.[12] When such photons [namely initial state radiation (ISR)] are included in the computation, the energy flowing in the first Z propagator of diagram 17 is not a constant any longer. Therefore, the prompt Z spectra would appear broader than those ones plotted here. Nevertheless, since the mean e^+e^- c.m. energy loss $\delta_{\sqrt{s}}$ due to ISR, is, e.g., $\approx 5\%$ at $\sqrt{s} = 500$ GeV [33], one can choose a window wide enough ($\approx \delta_{\sqrt{s}} \times \sqrt{s}$) to prevent complications due to such effects.[13] The effectiveness of this cut is clear from Table III, which presents the percentage of configurations that give an energy of the $b\bar{b}$ pair in a window of 25 GeV around the peak $E_{b\bar{b}}^{\max}$ for the above three $b\bar{b}ZZ$ subprocesses.

So, finally, requiring for the $e^+e^- \to b\bar{b}VV$ events to have energy of the $b\bar{b}$ pair in the above window around the maxima (which are $\approx$138(124)[105] GeV for $\sqrt{s} = 350$ GeV and $M_{H^0} = 185(210)[240]$ GeV, and $\approx$214(196)[168] GeV for $\sqrt{s} = 500$ GeV and $M_{H^0} = 210(250)[300]$ GeV for both the cases[14] $VV = ZZ, W^+W^-$) and calculating the corresponding percentage of events passing this cut (now for all the components of both the processes $e^+e^- \to b\bar{b}W^+W^-$ and $e^+e^- \to b\bar{b}ZZ$) leads to the final number of signal and background events, and their statistical significancies, given in Table IV. From which we deduce that an additional simple cut in $E_{b\bar{b}}$ increases the ratios $S/\sqrt{B}$ up to values such that Higgs boson detection should now be feasible everywhere just by adopting a pure missing mass analysis (i.e., without resorting to any identification of the decay products of the vector bosons).

Not even the inclusion of background contributions to the missing mass spectra coming from the "invisible" process $e^+e^- \to b\bar{b}\nu_l\bar{\nu}_l$ (with $l = e$, μ, and τ) should change our conclusions, as the corresponding distributions are nearly flat in the M_{H^0} ranges of interest, with rates that we verified to be $\lesssim 10^{-1}$ and $\lesssim 10^{-2}$ fb/GeV [34], for $\sqrt{s} = 350$ and 500 GeV, respectively, after the complete set of cuts in $M_{b\bar{b}}$, $\cos\theta_{b\bar{b}}$, and $E_{b\bar{b}}$. In fact, assuming the usual values of luminosity $\mathcal{L}$ and b-tagging efficiency ϵ_b, such numbers would give at most $\lesssim 10$ and $\lesssim 1$ background events, which would reduce the significancies in Table IV, but not enough to prevent the feasibility of Higgs boson detection.

TABLE III. Percentage of events with energy of the $b\bar{b}$ pair $E_{b\bar{b}}$ in the window $|E_{b\bar{b}}^{\max} - E_{b\bar{b}}| < 12.5$ GeV for the cases of a prompt Z^0, a H^0-decay Z^0, and a bremsstrahlung Z^0 (see in the text) at $\sqrt{s} = 350$ and 500 GeV for a selection of Higgs masses after the cuts: $|M_{Z^0} - M_{b\bar{b}}| < 10$ GeV and $|\cos\theta_{b\bar{b}}| < 0.8$.

M_{H^0} (GeV)	Prompt Z^0	H^0-decay Z^0	Bremsstrahlung Z^0
		$\sqrt{s} = 350$ GeV	
185	98%	0.63%	27%
210	99%	56%	70%
240	98%	36%	61%
		$\sqrt{s} = 500$ GeV	
210	98%	0.36%	18%
250	96%	23%	23%
300	91%	23%	22%
		$Z^0 \to b\bar{b}$	

[12]Even though photon emission can happen also off $b\bar{b}$ lines, however, this latter can easily be included in the invariant mass reconstructing the Z peak. So, we do not stress this case further, here.

[13]The inclusion of Linac energy spread and beamsstrahlung should not drastically change this strategy, at least for the "narrow" D-D and TESLA collider designs (see Ref. [33]).

[14]We do not reproduce here the figures for $e^+e^- \to b\bar{b}W^+W^-$, since they do not differ too much from Figs. 6 and 7: there the signal (various backgrounds) is (are) as narrow (broad with respect to the signal) as that (those) one(s) of $e^+e^- \to b\bar{b}ZZ$.

CONCLUSIONS

In summary, in this paper we studied the production of a heavy Higgs boson (with $2M_{W^\pm} < M_{H^0} < 2m_t$, where $m_t = 175$ GeV) and a Z through the Bjorken bremsstrahlung reaction $e^+e^- \to ZH^0$ at NLC energies, assuming $H^0 \to ZZ$ and $Z \to b\bar{b}$ and requiring a single b tagging for the Z detection. We have also studied all the irreducible background in $e^+e^- \to b\bar{b}ZZ$ events. We found that Higgs boson signals, which would be clearly detectable for $e^+e^- \to b\bar{b}ZZ$ on their own, still remain once we add (as needed for the missing mass anal-

TABLE IV. The expected number of signal and background events for $e^+e^- \to b\bar{b}Z^0Z^0$ and $e^+e^- \to b\bar{b}W^+W^-$ processes, added together, in the window $|M_{H^0} - M_{VV}| < 5$ GeV and their statistical significance at $\sqrt{s} = 350$ and 500 GeV for a selection of Higgs masses after the cuts: $|M_{Z^0} - M_{b\bar{b}}| < 10$ GeV, $|\cos\theta_{b\bar{b}}| < 0.8$, and $|E_{b\bar{b}} - E_{b\bar{b}}^{\max}| < 12.5$ GeV. We assume that only one b jet is tagged with efficiency $\epsilon_b = 1/3$. The luminosity is taken to be $\mathcal{L} = 10$ fb^{-1}. Numbers corresponding to the contribution of $e^+e^- \to b\bar{b}W^+W^-$ events are computed from Ref. [24] (assuming $m_t = 175$ GeV).

M_{H^0} (GeV)	Signals	Backgrounds	$S/\sqrt{B}$
		$\sqrt{s} = 350$ GeV	
185	47.43	18.60	11.00
210	32.08	5.97	13.13
240	14.79	1.40	12.50
		$\sqrt{s} = 500$ GeV	
210	23.91	0.14	62.84
250	15.87	1.54	12.79
300	7.42	5.09	3.29
		$\mathcal{L} = 10$ fb^{-1} $\epsilon_b = 1/3$	

ysis) this process to $e^+e^- \to b\bar{b}W^+W^-$, where $ZH^0 \to (b\bar{b})(W^+W^-)$ and which includes among the irreducible background the huge $t\bar{t} \to b\bar{b}W^+W^-$ production and decay. This was done only by imposing the following cuts on the $b\bar{b}$ system: $|\cos\theta_{b\bar{b}}| < 0.8$, $|M_{b\bar{b}} - M_Z| < 10$ GeV, and $|E_{b\bar{b}} - E_{b\bar{b}}^{\max}| < 12.5$ GeV, where $E_{b\bar{b}}^{\max}$ is the maximum in the energy spectrum of the $b\bar{b}$ pair, which is practically monoenergetic for the $b\bar{b}$ pair coming from a Z produced in the two-body Bjorken reaction. In particular, this latter cut turns out to be extremely useful in rejecting the $t\bar{t}$ background in $e^+e^- \to b\bar{b}W^+W^-$ events, thus avoiding further cuts based on the $t\bar{t}$ kinematics, which, although useful to the above aim, imply tagging the decay products of one of the two $W^{\pm}$'s.

ACKNOWLEDGMENTS

We are grateful to Tim Stelzer and Bas Tausk for useful suggestions and constructive discussions, to Alessandro Ballestrero and Ezio Maina for focusing our attention on some important aspects of the phenomenological analysis here presented, and to Ghadir Abu Leil for a careful reading of the manuscript. This work was supported in part by Ministero dell'Università e della Ricerca Scientifica.

[1] M. Veltman, Phys. Lett. **70B**, 253 (1977); B. W. Lee, C. Quigg, and G. B. Thacker, Phys. Rev. Lett. **38**, 883 (1977); Phys. Rev. D **16**, 1519 (1977).

[2] ALEPH Collaboration, Phys. Rep. **216**, 253 (1992); DELPHI Collaboration, Nucl. Phys. **B373**, 3 (1992); L3 Collaboration, Phys. Lett. B **303**, 391 (1993); OPAL Collaboration, *ibid.* **253**, 511 (1991).

[3] J. F. Guinon, H. E. Haber, G. L. Kane, and S. Dawson, *The Higgs Hunter Guide* (Addison-Wesley, Reading, MA, 1990).

[4] Proceedings of the "Large Hadron Collider Workshop," Aachen, 1990, edited by G. Jarlskog and D. Rein [Report Nos. CERN 90-10, ECFA 90-133, Geneva, 1990) (unpublished)].

[5] Proceedings of the "Summer Study on High Energy Physics in the 1990s," Snowmass, Colorado, 1988, edited by S. Jensen (unpublished); Proceedings of the "1990 Summer Study on High Energy Physics: Research Directions for the Decade," Snowmass, Colorado, 1990, edited by E. L. Berger (unpublished).

[6] J. F. Guinon and T. Han, Phys. Rev. D **51**, 1051 (1995).

[7] Proceedings of the ECFA workshop on LEP 200, Aachen, Germany, 1986, edited by A. Bohm and W. Hoogland [Report No. CERN 87-08 (unpublished)].

[8] *Physics and Experiments with Linear Colliders*, Proceedings of the Workshop, Sariselkä, Finland, 1991, edited by R. Orawa, P. Eerola, and M. Nordberg (World Scientific, Singapore, 1992).

[9] Proceedings of the workshop "e^+e^- Collisions at 500 GeV. The Physics Potential," Munich, Annecy, Hamburg, 1991, edited by P. M. Zerwas [DESY Report No. pub. 92-123A/B, August 1992 (unpublished)].

[10] Proceedings of the EFCA workshop on "e^+e^- Linear Colliders LC92," edited by R. Settles, Garmisch Partenkirchen, 1992 [Report Nos. MPI-PhE/93-14, ECFA 93-154 (unpublished)].

[11] Proceedings of the I Workshop on Japan Linear Collider (JLC), KEK 1989, KEK-Report No. 90-2 (unpublished); Proceedings of the II Workshop on Japan Linear Collider (JLC), KEK 1990, KEK-Report No. 91-10 (unpublished).

[12] C. Seez *et al.*, in Ref. [4].

[13] S. L. Glashow, D. V. Nanopoulos, and A. Yaldiz, Phys. Rev. D **18**, 1724 (1978).

[14] R. Kleiss, Z. Kunszt, and W. J. Stirling, Phys. Lett. B **253**, 269 (1991); SDC Collaboration, M. L. Mangano, note SSC-SDC-90-00113 (unpublished).

[15] R. Raitio and W. W. Wada, Phys. Rev. D **19**, 941 (1979); J. N. Ng and P. Zakarauskas, *ibid.* **29**, 876 (1984).

[16] J. F. Guinon, Phys. Lett. B **261**, 510 (1991); W. J. Marciano and F. E. Paige, Phys. Rev. Lett. **66**, 2433 (1991); A. Ballestrero and E. Maina, Phys. Lett. B **268**, 437 (1992); Z. Kunzst, Z. Trócsányi, and W. J. Stirling, *ibid.* **271**, 247 (1991); D. J. Summers, *ibid.* **277**, 366 (1992).

[17] V. Barger, K. Cheung, A. Djouadi, B. A. Kniehl, and P. M. Zerwas, Phys. Rev. D **49**, 79 (1994).

[18] J. D. Bjorken, Proceedings of the "Summer Institute on Particle Physics," [SLAC Report No. 198, 1976 (unpublished)]; B. W. Lee, C. Quigg, and H. B. Thacker, Phys. Rev. D **16**, 1519 (1977); J. Ellis, M. K. Gaillard, and D. V. Nanopoulos, Nucl. Phys. **B106**, 292 (1976); B. L. Ioffe and V. A. Khoze, Sov. J. Part. Nucl. **9**, 50 (1978).

[19] D. R. T. Jones and S. T. Petkov, Phys. Lett. **84B**, 440 (1979); R. N. Cahn and S. Dawson, *ibid.* **136B**, 196 (1984); K. Hikasa, *ibid.* **164B**, 351 (1985); G. Altarelli, B. Mele, and F. Pitolli, Nucl. Phys. **B287**, 205 (1987); B. Kniehl, DESY Report No. 91-128, 1991 (unpublished).

[20] V. Barger, K. Cheung, B. A. Kniehl, and R. J. Phillips, Phys. Rev. D **46**, 3725 (1992).

[21] K. Higawara, J. Kanzaki, and H. Murayama, Durham. Univ. Report No. DTP-91-18, 1991 (unpublished).

[22] "Solenoidal Detector Collaboration Technical Design Report," E. L. Berger *et al.*, Report Nos. SDC-92=201, SSCL-SR-1215, 1992 (unpublished).

[23] J. Dai, J. F. Gunion, and R. Vega, Phys. Rev. Lett **71**, 2699 (1993); Phys. Lett. B **315**, 355 (1993).

[24] A. Ballestrero, E. Maina, and S. Moretti, Phys. Lett. B **335**, 460 (1994).

[25] H. Borner and P. Grosse-Wiesmann, in Ref. [9].

[26] P. Grosse-Wiesmann, D. Haidt, and H. J. Schrieber, in Ref. [9].

[27] P. Janot, in Ref. [9].

[28] K. Hagiwara and D. Zeppenfeld, Nucl. Phys. **B274**, 1 (1986).

[29] K. Fujikawa, B. W. Lee, and A. I. Sanda, Phys. Rev. D **6**, 2923 (1972); C. Becchi, A. Rouet, and B. Stora, Commun. Math. Phys. **42**, 127 (1975); Ann. Phys. **98**, 287 (1976); B. W. Lee, C. Quigg, and H. B. Thacker, Phys. Rev. D **16**, 1519 (1977); M. S. Chanowitz and M. K. Gaillard, Nucl. Phys. **B261**, 379 (1985); G. J. Gounaris, R. Kögerler, and H. Neufeld, Phys. Rev. D **34**, 3257 (1986).

[30] T. Stelzer and W. F. Long, Comp. Phys. Commun. **81**, 357 (1994).

[31] E. Murayama, I. Watanabe, and K. Hagiwara, HELAS: HELicity Amplitude Subroutines for Feynman Diagram Evaluations, KEK Report No. 91-11, January 1992 (unpublished).
[32] G. P. Lepage, J. Comput. Phys. **27**, 192 (1978).
[33] T. Barklow, P. Chen, and W. Kozanecki, in Ref. [9].
[34] S. Moretti, Report Nos. DFTT 40/95, DTP/95/58, June 1995 (unpublished).